LIMNOLOGY and OCEANOGRAPHY

ASLO

Limnol. Oceanogr. 9999, 2024, 1–14

doi: 10.1002/lno.12533

Omnivorous summer feeding by juvenile Antarctic krill in coastal waters

John A. Conroy [1*,a] **Deborah K. Steinberg** [1] **Schuyler C. Nardelli** [2,b] **Oscar Schofield** [2]

[1]Virginia Institute of Marine Science, William & Mary, Gloucester Point, Virginia, USA
[2]Department of Marine and Coastal Sciences, Rutgers University's Center for Ocean Observing Leadership, Rutgers, The State University of New Jersey, New Brunswick, New Jersey, USA

Abstract

The Antarctic krill *Euphausia superba* is often considered an herbivore but is notable for its trophic flexibility, which includes feeding on protistan and metazoan zooplankton. Characterizing krill trophic position (TP) is important for understanding carbon and energy flow from phytoplankton to vertebrate predators and to the deep ocean, especially as plankton composition is sensitive to changing climate. We used repeated field sampling and experiments to study feeding by juvenile krill during three austral summers in waters near Palmer Station, Antarctica. Our approach was to combine seasonal carbon budgets, gut fluorescence measurements, imaging flow cytometry, and compound-specific isotope analysis of amino acids. Field measurements coupled to experimentally derived grazing functional response curves suggest that phytoplankton grazing alone was insufficient to support the growth and basal metabolism of juvenile krill. Phytoplankton consumption by juvenile krill was limited due to inefficient feeding on nanoplankton (2–20 μm), which constituted the majority of autotrophic prey. Mean krill TP and the metazoan dietary fraction increased in years with higher mesozooplankton biomass, which was not coupled to phytoplankton biomass. Comparing TP estimates using $\delta^{15}N$ of different amino acids indicated a substantial and consistent food-web contribution from heterotrophic protists. Phytoplankton, metazoans, and heterotrophic protists all were important contributors to a diverse krill diet that changed substantially among years. Juvenile krill fed mostly on heterotrophic prey during summer near Palmer Station, and this food web complexity should be considered more broadly throughout the changing Southern Ocean.

The Antarctic krill *Euphausia superba* (hereafter "krill") contributes to Southern Ocean carbon export (Gleiber et al. 2012; Belcher et al. 2019), supports large populations of vertebrate predators (Trathan and Hill 2016), and is targeted by the region's largest commercial fishery (Nicol and Foster 2016). Krill are omnivores and assessing their trophic role is challenging, although phytoplankton typically are considered their primary prey (Hewes et al. 1985; Price et al. 1988; Schmidt and Atkinson 2016). Phytoplankton biomass and composition change with regional sea ice coverage (Montes-Hugo et al. 2009; Brown et al. 2019), but the implications of changing prey composition remain unclear for krill. Increased reliance on heterotrophic prey likely would decrease the proportion of phytoplankton production that is vertically exported or made available to krill predators, as organic matter is lost via respiration with each trophic step between phytoplankton and krill.

Krill have a lifetime of ~ 6 yr, and juvenile (age-class 1) krill exhibit particular trophic flexibility. In years of successful recruitment, juveniles dominate the krill population and predator diet composition, apparently due to strong bottom-up forcing (Saba et al. 2014). However, the number of trophic transfers between phytoplankton and vertebrate predators remains uncertain, because krill feed on a combination of phytoplankton, copepods, and protistan grazers (Schmidt et al. 2006). Juvenile krill generally occupy lower trophic positions (TPs) than adults (Polito et al. 2013; Schmidt et al. 2014), and higher-productivity continental shelf regions such as the West Antarctic Peninsula (WAP) are associated with faster krill

*Correspondence: jaconroy@ucsc.edu

Additional Supporting Information may be found in the online version of this article.

[a]Present address: Ocean Sciences Department, University of California, Santa Cruz, Santa Cruz, California, USA
[b]Present address: California Water Science Center, U.S. Geological Survey, Sacramento, California, USA

Author Contribution Statement: J.A.C., D.K.S., and O.S. conceived the study. J.A.C. and S.C.N. acquired and analyzed data. J.A.C. produced figures and wrote the manuscript with contributions from all co-authors.

growth, presumably due to diatom-dominated diets (Atkinson et al. 2006; Schmidt et al. 2014). However, phytoplankton ingestion (i.e., grazing) rates are insufficient to satisfy minimum respiratory requirements, let alone growth, for juveniles during summer along the WAP (Bernard et al. 2012). We thus investigated the diet composition of juvenile krill, which must feed on animals to an unknown extent.

In this study, we employed multiple methods to examine the dietary flexibility of juvenile krill during productive summer months at the coastal WAP. By focusing on the juvenile life stage in a productive season and location (Clarke et al. 2008; Vernet et al. 2008), we expected this study to provide an upper-limit estimate for phytoplankton contributions to krill diet. Using a combination of semiweekly field sampling and a series of 24-h incubation experiments, our main objectives were to: (1) determine seasonal growth and carbon requirements for juvenile krill; (2) understand grazing dynamics, including mass-specific grazing rates and size selectivity; (3) create a carbon budget for juvenile krill to evaluate the contribution of major prey groups; and (4) assess interannual changes in TP and dietary composition. Our results quantify the diverse juvenile krill diet and show these animals rely upon heterotrophic prey even in a season and location favorable for herbivory.

Materials and methods

Krill collection, seasonal growth, and carbon requirement

We collected krill southwest of Anvers Island, near Palmer Station (64°46′S, 64°03′W), as part of the Palmer Antarctica Long-Term Ecological Research (PAL LTER) program. Our sampling spanned November to March over three field seasons: 2017–2018, 2018–2019, and 2019–2020 (Conroy et al. 2023). We collected krill aboard a rigid-hulled inflatable boat using two net types: a 1-m square frame, 700-μm mesh Metro net and a 1-m diameter, 200-μm mesh ring net. We sampled from 0 to 50 m at PAL LTER Sta. B (~ 1 km from Palmer Station, bottom depth ~ 70 m) and Sta. E (~ 5 km from Palmer Station, bottom depth ~ 160 m) twice per week (Supplementary Fig. S1) (Conroy et al. 2023) and less consistently at other fixed sampling locations or by targeting krill swarms identified by echosounder.

The daily length mode for juvenile krill was used to calculate a seasonal growth curve. We measured krill to the nearest 0.01 mm using Standard Length 1 (Mauchline 1980). Krill collected in multiple tows on the same date were pooled for modal analysis, and only dates with > 20 measured krill were included (median: 106 krill measured per date; range: 21–431). Lengths were binned into 1-mm intervals, and a kernel density estimate was fit to each daily length–frequency distribution using the function "density" in R (R Core Team 2021) (Supplementary Methods; Supplementary Figs. S2–S4). The length-at-date data ($n = 55$ d) were fit to a Von Bertalanffy growth model using the function "nls" in R. The resulting model fit exhibited homoscedasticity, and the residuals were normally distributed.

The Von Bertalanffy model fit was then used to calculate a daily carbon budget for juvenile krill. Length (mm) was converted to dry weight (mg) as in Ryabov et al. (2017). Carbon was assumed to constitute 46.3% of dry weight, which was the mean of values for juvenile krill collected in December (Ikeda and Bruce 1986) and February (Färber-Lorda et al. 2009). Daily growth rate (G; mg C d^{-1}) for each day n was calculated as: $G_n = ((CW_{n+1} - CW_{n-1})/2)$, where CW is carbon weight. The minimum daily respiratory requirement (mg C d^{-1}) was calculated from dry weight as in Holm-Hansen and Huntley (1984). Minimum carbon ingestion was calculated as the sum of daily growth and respiration, divided by an assimilation efficiency of 85%. Prior studies report mean assimilation efficiencies of 84–88% for krill (Meyer et al. 2003; Fuentes et al. 2016).

Chlorophyll *a* grazing: Gut fluorescence

Cholorophyll *a* (Chl *a*) content in field-collected krill was measured using the gut fluorescence technique. Individual krill were removed immediately from the catch, measured for length and frozen in liquid N_2. We froze 3–5 individuals of each distinct size class per tow. Samples were stored at −80°C until analysis. Gut pigments were extracted from whole animals in 90% acetone for at least 48 h at −20°C to ensure complete pigment extraction without homogenization (Båmstedt et al. 2000; Pakhomov and Froneman 2004). Samples were centrifuged and returned to room temperature for determination of pigment concentration before and after acidification using a Turner 10 AU fluorometer.

Grazing rate (μg Chl *a* equivalent $ind.^{-1}$ h^{-1}) was calculated as the product of gut pigment content (sum of phaeopigments and Chl *a*, in μg) and gut evacuation rate (h^{-1}). We used a value of 1.48 h^{-1} for the gut evacuation rate, the mean of experimentally derived rates (range 1.12–1.90 h^{-1}) for juvenile krill during summer in WAP shelf waters (Bernard et al. 2012). Hourly grazing rate was multiplied by 24 h to calculate daily grazing rate (μg Chl *a* equiv. $ind.^{-1}$ d^{-1}). Grazing rate and mass-specific grazing rate (μg Chl *a* equiv. mg DW^{-1} d^{-1}) were log-transformed for linear regression to test for relationships with standard length and log-transformed Chl *a* concentration. Chl *a* concentration was measured via fluorometric analysis of bottle samples and integrated 0–50 m (Schofield et al. 2017; Conroy et al. 2023).

Chlorophyll *a* grazing: Functional response

We conducted feeding incubations with juvenile krill to measure clearance rate (i.e., the rate at which a predator sweeps a volume of water clear of a prey type) and grazing rate on natural plankton communities. Krill were collected from the upper 50 m in net tows using a non-filtering cod end, transferred to 20-liter buckets of whole seawater, and

acclimated for 24 h to experimental conditions in an outdoor flow-through incubator at ambient temperature and light conditions (screened for ~ 33% light transmittance). We collected whole seawater the following day from the depth of the Chl *a* maximum to fill the experimental buckets and took initial samples for Chl *a* and particle size distribution. Chl *a* samples were filtered through Whatman GF/F filters and frozen at −80°C until analysis.

Four to 10 krill were transferred to each of 4–6 experimental replicates. An additional 4–6 replicates were maintained as controls without krill. All experimental buckets were gently stirred on average every 2 h to re-suspend cells. Experiments ran for 24 h, after which final samples for Chl *a* and particle size distribution were collected from each replicate. Replicates were excluded if krill were dead or inactive.

In one case, experimental seawater was diluted with 0.2-μm filtered seawater so that treatments of 100%, 30%, and 10% whole seawater were incubated on a single date. These concentrations were treated as separate experimental units, because measuring clearance rate at low prey concentrations is critical for distinguishing functional response types (i.e., consumption as a function of prey density) (Kiørboe et al. 2018). In this case, three krill replicates and a single control were maintained at each concentration.

Clearance and grazing rates were calculated to determine the krill feeding functional response. Clearance rate (L ind.$^{-1}$ d^{-1}) was calculated according to Frost (1972), and negative clearance rates (14 out of 67 total replicates) were excluded from further analysis (Supplementary Methods). Grazing rate was calculated as the product of clearance rate and initial Chl *a* concentration (Marin et al. 1986). Type II (Holling 1965) and type III (Kiørboe et al. 1982) functional response curves were fit using the "'nls"' function in R. These two functional responses differ at low prey concentrations, with clearance rate peaking when prey is scarce for a type II response but declining under such conditions for a type III response. The experimental data better fit a type III functional response due to declining clearance rates at low Chl *a* concentrations.

The experimentally derived type III functional response model allowed estimation of grazing rates based on repeated field observations of Chl *a* concentration. In situ Chl *a* concentration was measured twice per week at PAL LTER Sta. B on 0–60 m downcasts with a Wet Labs ECO fluorometer. Fluorescence data were binned into 1-m depth intervals prior to identifying the maximum Chl *a* concentration (chl_{max}) for each vertical profile. We solved for Chl *a* grazing using the chl_{max} from each vertical profile.

Phytoplankton carbon

To evaluate phytoplankton grazing in juvenile krill carbon budgets, we utilized historical field data to calculate two different regression fits for converting Chl *a* to phytoplankton carbon (C_{phyto}; μg C L^{-1}) (Supplementary Methods). The two chlorophyll-to-carbon regression fits were used to calculate high and low C_{phyto} values from experiments and field observations. All calculations were repeated with both the high and low C_{phyto} regression fits to define an envelope of feasible values (Supplementary Methods). The contemporary Sta. B C_{phyto} time-series data were used to repeatedly solve the functional response equations, resulting in seasonal time series of high and low C_{phyto} grazing for each field season. Finally, we integrated the high and low estimates of C_{phyto} grazing rates each year from 01 December to 28 February and divided by minimum required carbon ingestion over the same period to evaluate the dietary contribution of phytoplankton.

Size-selective grazing

Initial and final experimental particle size distributions were derived from 5-mL samples analyzed with an Imaging FlowCytobot (Olson and Sosik 2007). Images included both photosynthetic and non-photosynthetic particles, because the instrument was set to trigger with a side scatter or fluorescence threshold. For three experiments, samples were preserved in 50% glutaraldehyde, frozen in liquid N_2, and stored at −80°C until analysis. Preservation may lead to underestimation of total biovolume and cell abundance, but relative changes (as considered here within experiments) were consistent in a comparison of live and preserved samples (Nardelli et al. 2023). The proportional contribution of different taxonomic groups was also similar in live and preserved comparisons. Particle images were processed according to Sosik and Olson (2007). All particles with a diameter of 4–40 μm were categorized into 13 discrete bins based on equivalent spherical diameter, and all bin widths were equal on a logarithmic scale. The biovolume concentration (μm^3 L^{-1}) was summed within each bin for every sample. Clearance rates for each prey size bin were calculated according to Frost (1972), and negative values were excluded.

Compound-specific isotope analysis of amino acids

Krill from 4 to 10 sampling dates during each season were frozen at −80°C at Palmer Station and processed for compound-specific isotope analysis of amino acids (CSIA-AA). Each sample consisted of 6–78 individuals collected on the same day. We measured krill length, dissected the 3rd and 4th abdominal segments, and removed the exoskeleton (Schmidt et al. 2004). Each pooled daily sample was freeze-dried for 24 h, then homogenized, and weighed (range 5.7–34.5 mg). Samples were processed at the Stable Isotope Facility at the University of California, Davis for CSIA-AA of ^{15}N following Walsh et al. (2014) and Yarnes and Herszage (2017) (Supplementary Methods).

Trophic position and dietary composition

CSIA-AA provides an internal index for TP, accounting for asynchronous changes in the isotopic signature of primary producers and consumers (Schmidt et al. 2004). The δ^{15}N (ratio of ^{15}N/^{14}N) of "trophic" amino acids increases

substantially with each trophic step (McMahon and McCarthy 2016). In contrast, N fractionation is limited in "source" amino acids, which retain $\delta^{15}N$ values similar to a food web's baseline. The difference in $\delta^{15}N$ between "trophic" and "source" amino acids within a consumer is used to determine TP.

Trophic fractionation within a food web generally declines after the initial transfer from phytoplankton to zooplankton (McMahon and McCarthy 2016; Décima et al. 2017). Therefore, multiple trophic enrichment factors (TEFs) are used to account for this variability. TEFs represent the $\delta^{15}N$ change in a trophic amino acid normalized to the $\delta^{15}N$ change in a source amino acid for a given trophic step. We thus calculate krill TP according to Hoen et al. (2014):

$$TP = \frac{\delta^{15}N_{trophic} - \delta^{15}N_{source} - \beta - TEF_{herbivory}}{TEF_{carnivory}} + 2$$

where β is the mean difference between $\delta^{15}N$ values of the trophic and source amino acids within primary producers, and $TEF_{herbivory}$ and $TEF_{carnivory}$, respectively, are the TEFs for herbivorous and carnivorous trophic transfers.

We calculated TP separately using glutamic acid (Glu) and alanine (Ala) as trophic amino acids. Both glutamic acid and alanine enrich through metazoans, but only alanine enriches through protistan grazers (Gutiérrez-Rodríguez et al. 2014; Décima et al. 2017). Phenylalanine (Phe) was the source amino acid in both cases. We used β and $TEF_{herbivory}$ values from Chikaraishi et al. (2009): $\beta_{Glu} = 3.4‰$; $\beta_{Ala} = 3.2‰$; $TEF_{herbivory_{Glu}} = 7.6‰$; $TEF_{herbivory_{Ala}} = 5.7‰$. For $TEF_{carnivory}$, we used lower values from Décima and Landry (2020): $TEF_{carnivory_{Glu}} = 6.1‰$ and $TEF_{carnivory_{Ala}} = 4.5‰$.This approach enables characterization of a range of feasible dietary contributions from major prey groups. We used the mean krill TP_{Glu} and TP_{Ala} values from each field season for this exploratory exercise. We calculated the dietary fractions of metazoans and heterotrophic protists as in Décima and Landry (2020) (Supplementary Methods). Calculating these dietary fractions involves multiple unmeasured parameters and should be considered experimental. The phytoplankton dietary fraction was a closure term (i.e., total diet composition must sum to 100%) for comparison with the same metric calculated from the seasonal carbon budget.

Prey biomass

For comparison with interannual patterns in krill trophic role, metazoan and phytoplankton prey were quantified from time-series sampling at PAL LTER Stas. B and E across the study years. Mesozooplankton (0.2–2 mm) biomass, an indicator of metazoan prey availability, was measured twice weekly using a 1-m diameter, 200-μm mesh ring net from 0 to 50 m (Conroy et al. 2023). Mesozooplankton dry weight density (g m^{-3}) was depth-integrated to 50 m (g m^{-2}). Phytoplankton biomass (Chl *a*) was measured via fluorometric analysis as described above (Schofield et al. 2017; Conroy et al. 2023).

Results

Seasonal growth and carbon requirement

November to March was a period of rapid growth and increasing carbon demand for juvenile krill. The length mode increased from 13–16 mm in early November to 26–30 mm in late February (Fig. 1a). Length-based growth rate declined from 0.21 mm d^{-1} on 06 November to 0.082 mm d^{-1} on 03 March. The mean length-based growth rate over that period was 0.13 mm d^{-1}. Carbon-based growth rate (mean = 0.14 mg C d^{-1}) followed the opposite seasonal trend, increasing from 0.07 mg C d^{-1} on 06 November to a maximum of 0.17 mg C d^{-1} on 23 February (Fig. 1b). More carbon was required for growth than for respiration until 22 December, but after 20 February daily growth equaled < 50% of the respiratory demand. Minimum carbon ingestion increased seasonally from 0.12 mg C d^{-1} (8.1% of body C) to 0.65 mg C d^{-1} (3.6% of body C) (Fig. 1c).

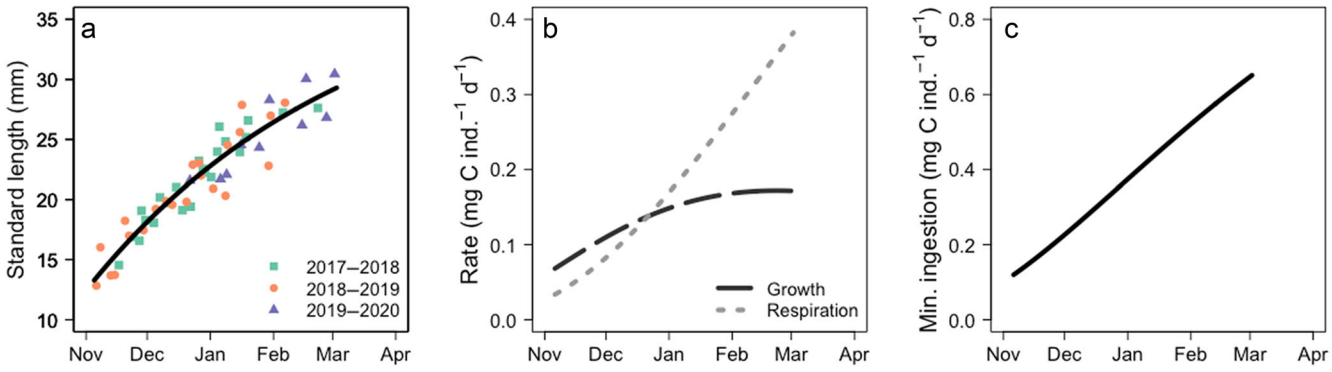

Fig. 1. Seasonal time series of juvenile krill growth and carbon demand. (**a**) Daily length modes (colored points) and the Von Bertalanffy model fit (black line), (**b**) modeled daily growth (dashed black line) and respiration rates (dotted gray line), and (**c**) modeled minimum daily carbon ingestion are plotted from November to March for juvenile krill near Palmer Station using data from 3 successive years.

Chlorophyll *a* grazing

As measured by the gut fluorescence method, the mean Chl *a* grazing rate was 0.73 μg Chl *a* ind^{-1} d^{-1} (range: 0.08–2.6 μg ind^{-1} d^{-1}; $n = 48$ tows). Seasonal patterns in grazing rate changed among years (Fig. 2a), but the mean grazing rate was not significantly different between years ($\log_{10}$-transformed ANOVA: $F_{2,45} = 1.4$; $p = 0.26$). The mean grazing rate increased with depth-integrated Chl *a* concentration (linear regression: $t = 2.5$; $p = 0.016$; $r^2 = 0.12$) but was not significantly correlated with the mean length of krill (linear regression: $t = 1.1$; $p = 0.26$). The mass-specific grazing rate was more strongly related with Chl *a* concentration (Fig. 2b) and declined by an order of magnitude as krill grew from 11 to 29 mm (Fig. 2c) (multiple linear regression: $|t| \geq 3.0$; $p \leq 0.005$; $r^2 = 0.47$).

Chl *a* grazing in experimental feeding incubations exceeded gut fluorescence measurements and fit a type III functional response. Mean initial Chl *a* ranged from 0.10 to 3.1 μg L^{-1} across 13 experiments, and mean grazing rates ranged from 0.11 to 4.0 μg ind^{-1} d^{-1} (Fig. 3a). According to this functional response curve, the Chl *a* grazing rate was 2.6 μg ind^{-1} d^{-1} (i.e., equal to the maximum rate from gut fluorescence) when Chl *a* concentration was 1.6 μg L^{-1}. At the high end of our experimental range, a Chl *a* concentration of 3.0 μg L^{-1} coincided with a modeled grazing rate of 3.6 μg ind^{-1} d^{-1}. The type III functional response fit indicated that clearance rate reached a maximum of 1.8 L ind^{-1} d^{-1} when Chl *a* was 0.98 μg L^{-1} and then gradually declined as Chl *a* increased (Fig. 3b).

The Chl *a* grazing time series calculated from the experimental functional response and in situ chl$_{max}$ measurements yielded higher values than the gut fluorescence method. Across three field seasons, chl$_{max}$ at PAL LTER Sta. B ranged from 0.2 to 19.1 μg L^{-1} over 104 sampling dates and was below our maximum experimental concentration of 3.1 μg L^{-1} for 76% of observations (Supplementary Fig. S7). Chl$_{max}$ was significantly higher in 2018–2019 (median: 2.8 μg L^{-1}) than in 2017–2018 (1.3 μg L^{-1}) or 2019–2020 (1.5 μg L^{-1}) ($\log_{10}$-transformed ANOVA: $F_{2,101} = 13.9$; $p < 0.00001$; Tukey's Honestly Significant Difference: $p < 0.005$). The mean Chl *a* grazing rate from the functional response model was 2.8 μg ind^{-1} d^{-1} (Fig. 4), which exceeded the highest daily grazing rate from the gut fluorescence method (2.6 μg ind^{-1} d^{-1}). Mean Chl *a* grazing was 3.4 μg ind^{-1} d^{-1} in 2018–2019 and significantly higher compared to 2.2 and 2.6 μg ind^{-1} d^{-1}, respectively, in 2017–2018 and 2019–2020 (ANOVA: $F_{2,101} = 14.5$; $p < 0.00001$; Tukey's HSD: $p < 0.004$).

Phytoplankton carbon grazing

The high and low seasonal C_{phyto} grazing scenarios differed by a factor of 2, and both scenarios indicate that autotrophic prey were inadequate to satisfy juvenile krill dietary needs during summer near Palmer Station. The seasonally integrated minimum ingestion to support growth and respiration from 01 December to 28 February was 39.3 mg C ind^{-1} (Fig. 5). In comparison, the estimates of C_{phyto} grazing for that same period ranged from 5.5 to 13.8 mg C ind^{-1}. Accordingly, phytoplankton accounted for only 14–35% of the minimum carbon ingestion required by juvenile krill during our three summer field seasons. This deficit was the result of consistent phytoplankton grazing while krill grew larger and respiratory requirements increased (Supplementary Fig. S9). As such, daily phytoplankton rations declined seasonally and were consistently < 1% krill body C d^{-1} by mid-February (Supplementary Fig. S10).

Size-selective grazing

Imaging flow cytometry from 11 feeding experiments revealed a mismatch between the size-selectivity of juvenile krill and the size distribution of their potential prey, with phytoplankton biomass concentrated within small cells that krill consumed inefficiently. The mean clearance rate increased from ~ 1 L ind^{-1} d^{-1} on particles sized 4–12 μm to 4.5 L ind^{-1} d^{-1} on particles 34–40 μm, the largest size bin in

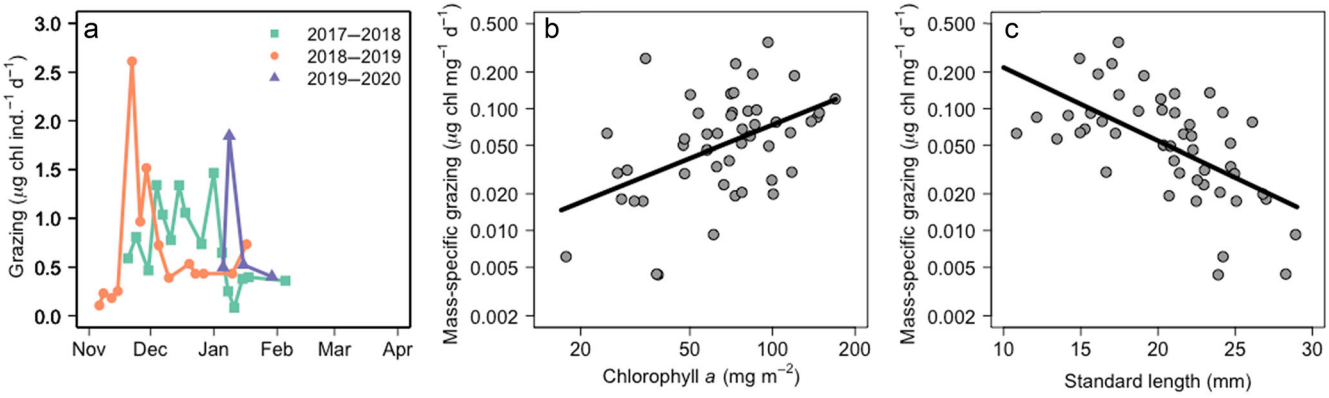

Fig. 2. Gut fluorescence-based estimates of Chl *a* grazing by juvenile krill. (**a**) Time series of daily mean Chl *a* grazing is plotted for three field seasons. (**b**) Depth-integrated Chl *a* concentration and (**c**) length of krill are plotted against mass-specific grazing. Log–log and log–linear regression fits are plotted in (**b**) and (**c**), respectively.

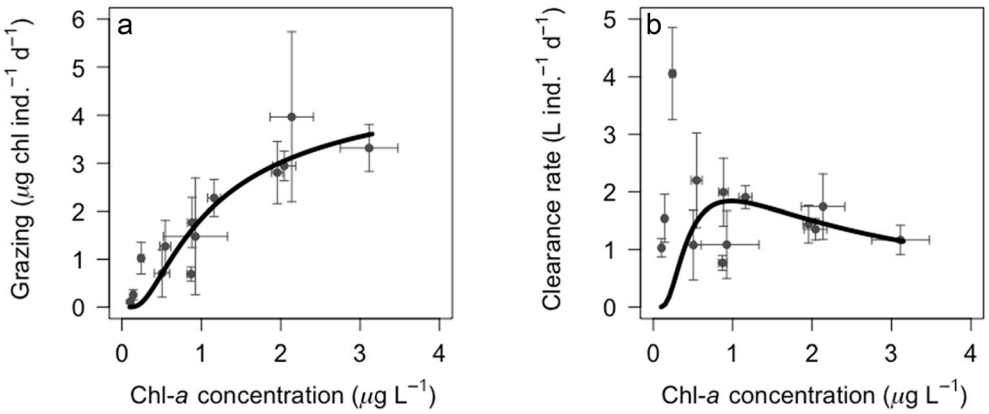

Fig. 3. Functional response of juvenile krill feeding on phytoplankton (Chl *a*). Mean (**a**) grazing and (**b**) clearance rates are plotted against mean initial Chl *a* concentration for 13 experiments. Error bars indicate one standard error, $n = 3$–6 replicates per experiment. Model fit: Chl *a* grazing $= 0.98 \times 1.84 \times e^{1-0.98/\text{Chl } a \text{ concentration}}$.

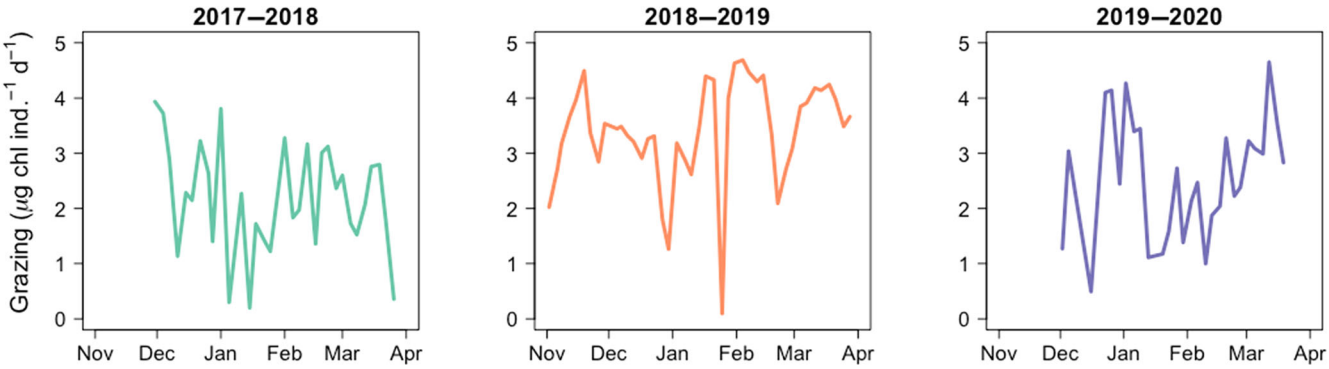

Fig. 4. Juvenile krill Chl *a* grazing time series calculated using the functional response model and in situ Chl *a* maxima during the 2017–2018, 2018–2019, and 2019–2020 field seasons.

our analysis (Fig. 6a). In contrast, 5–12 μm particles accounted for 62% of mean initial prey biovolume in our feeding experiments (Fig. 6b). The variability in total phytoplankton biomass across experiments was likely due to changes in 5–12 μm cells, the biovolume of which was more variable than that of larger size classes.

Trophic position and dietary composition

TP estimates using the δ^{15}N values of amino acids support the importance of heterotrophic prey for juvenile krill during summer. The source amino acid phenylalanine δ^{15}N values ranged from −0.7‰ to 2.7‰ while the δ^{15}N values of the trophic amino acids glutamic acid and alanine ranged from 12.0‰ to 16.3‰ and 12.6‰ to 18.2‰, respectively (Fig. 7; Supplementary Table S1). TP_{Glu} (mean $= 2.3 \pm 0.2$ standard deviation) was significantly lower than TP_{Ala} (mean $= 3.1 \pm 0.4$) (paired *t*-test: $t = 16$; df $= 22$; $p = 2.2 \times 10^{-13}$) (Fig. 8a,b). This difference presumably was due to trophic steps through heterotrophic protists, which TP_{Glu} does not detect. The mean difference in TP estimates between the two methods was 0.7 and did not change significantly between years (ANOVA: $F_{2,20} = 1.2$; $p = 0.32$), indicating that heterotrophic protists were a substantial, consistent trophic link between phytoplankton and juvenile krill. In contrast, mean TP_{Glu} and TP_{Ala} were both 0.2–0.5 trophic steps lower in 2017–2018 compared to 2018–2019 and 2019–2020 (ANOVA: $F_{2,20} > 5.2$; $p < 0.02$; Tukey's HSD: $p < 0.05$) (Fig. 8a,b), suggesting that the trophic contribution of metazoan prey increased in the latter 2 yr. This interannual pattern matched changes in mesozooplankton biomass, which also was lowest in 2017–2018 ($\log_{10}$-transformed ANOVA: $F_{2,114} > 6.8$; $p < 0.002$; Tukey's HSD: $p < 0.02$) (Fig. 8c).

Our exploratory stable isotope approach attributed on average approximately one-third of krill dietary composition each to phytoplankton, heterotrophic protists, and metazoans (Table 1). The isotope-derived phytoplankton dietary fraction exceeded that from the carbon budget in 2017–2018, but mean values of 22–27% agreed across methods in the final 2 study years (Table 1). The carbon budget did not reflect interannual changes evident in the stable isotope data. High and low estimates of phytoplankton and heterotrophic protist dietary fraction differed by 30–41% within each year,

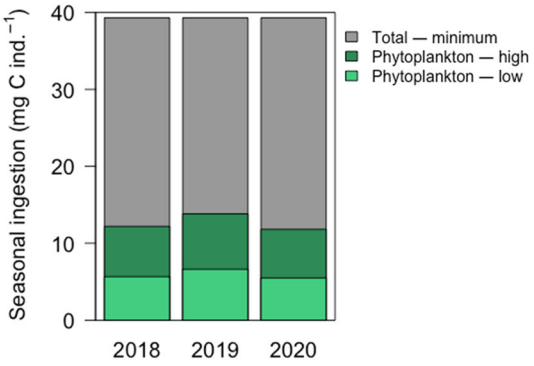

Fig. 5. Seasonally integrated juvenile krill carbon ingestion for 3 successive years. The modeled minimum carbon ingestion from 01 December to 28 February (gray) is constant at 39.3 mg C ind^{-1} across years and is derived from the combined krill length time series. Functional response models were paired with phytoplankton carbon concentration estimates to calculate time series for high (dark green) and low (light green) estimates of phytoplankton grazing for each year.

indicating substantial uncertainty. This exercise revealed it was unlikely for a single major prey group to dominate the juvenile krill diet in any year, with all annual estimates falling below 63% (Table 1). Phytoplankton, heterotrophic protists, and metazoans each had the highest mean dietary fraction estimate for a single year, indicating that the relative balance among prey groups changed. The interannual changes were greatest (and inversely related) for phytoplankton and metazoan dietary fraction. The shift toward a larger metazoan dietary fraction coincided with years of increased mesozooplankton prey. Changes in Chl *a* were not consistent with krill diet alteration. Overall, this analysis suggests juvenile krill utilized a diverse and changing suite of prey across 3 yr.

Discussion

Seasonal growth and carbon requirement

Summer is a period of rapid growth for juvenile krill, and our measured growth rates appear robust when compared with other methods. Mean daily growth rate during January and February was 0.11 mm d^{-1}. Similarly, a length-frequency approach utilizing net surveys from 1992 to 2008 in the northern Antarctic Peninsula reported mean growth of ~ 0.1 mm d^{-1} between January and February for 20–30 mm krill (Shelton et al. 2013). A meta-analysis of instantaneous growth rate data found a seasonal decline in daily growth from ~ 0.2 mm d^{-1} in early summer to < 0.1 mm d^{-1} by early autumn (Kawaguchi et al. 2006), similar to the pattern from our Von Bertalanffy model fit. Given the agreement between these independent methods and studies, our length-based seasonal growth curve is a reasonable basis from which to infer minimum carbon demand.

Our calculated minimum daily carbon ingestion was conservative, because it accounted only for respiration and somatic growth. Minimum ingestion rates of 4–8% krill body

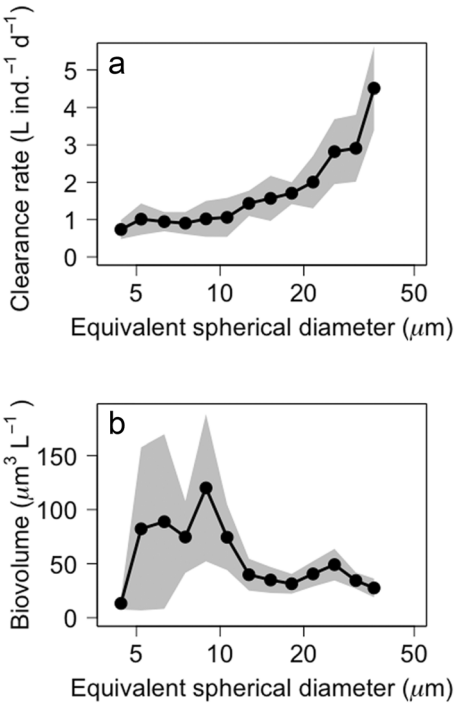

Fig. 6. Size-selective grazing by juvenile krill. Equivalent spherical diameter of particles vs. (**a**) mean clearance rate and (**b**) initial particle biovolume. Based on particle equivalent spherical diameter, potential prey particles were binned into 13 bins of equal width on a logarithmic scale. Shading indicates two standard errors, n = 9–11 experimental means.

carbon d^{-1} found in this study are well below the highest reported daily rations of ~ 20% body carbon d^{-1} (Clarke et al. 1988; Atkinson et al. 2006). We assumed investment in reproduction was negligible, because krill typically do not reach maturity until at least 32 mm (age-class 2) (Siegel and Loeb 1994; Reiss 2016). Excretion, however, was not calculated and may be substantial. Experimentally measured dissolved organic carbon (DOC) release by krill during January and February is 202 μmol g^{-1} h^{-1} (Ruiz-Halpern et al. 2011), but the distinct release mechanisms of assimilated vs. unassimilated DOC are unassessed for krill, and therefore excretion rates remain unknown. The respiratory cost of swimming also is not trivial (Swadling et al. 2005) but similarly is excluded from our carbon budget due to uncertainty. As a consequence of our conservative ingestion estimate, phytoplankton may account for a smaller dietary fraction than the 14–35% reported here.

Phytoplankton grazing

Repeated gut fluorescence measurements provided valuable insight into the regional variability, allometry, and functional response of krill grazing. Chl *a* grazing rates were intermediate compared to those from two previous studies of juvenile krill using gut fluorescence. Our values (0.1–2.6 μg ind^{-1} d^{-1}) were lower than those measured by Bernard et al. (2012) during January along the WAP (1.4–6.6 μg ind^{-1} d^{-1}). Grazing rates

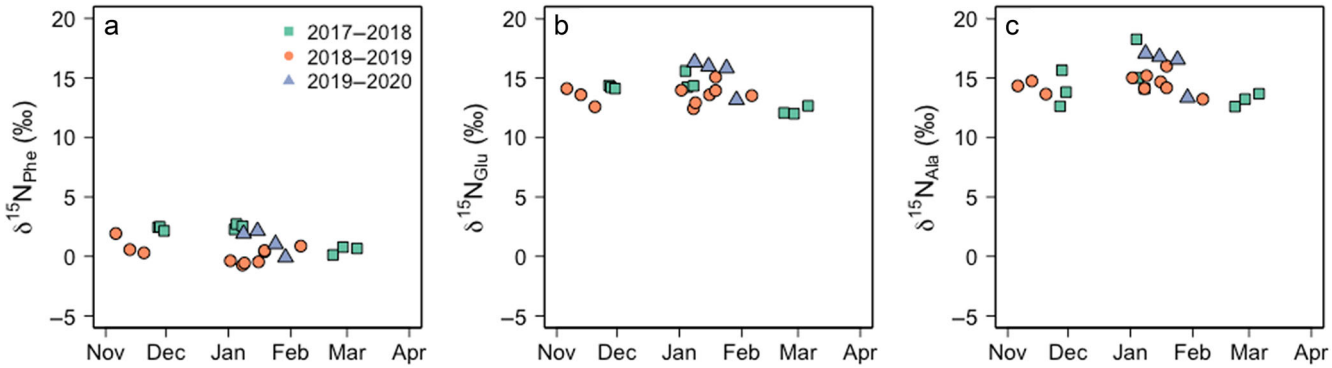

Fig. 7. Amino acid $\delta^{15}N$ values in the abdominal muscle of juvenile krill during three consecutive field seasons. Amino acids are (**a**) phenylalanine, (**b**) glutamic acid, and (**c**) alanine. Points indicate the mean of duplicate analytical injections. The average standard deviations for phenylalanine, glutamic acid, and alanine duplicates were 0.4‰, 0.2‰, and 0.2‰, respectively.

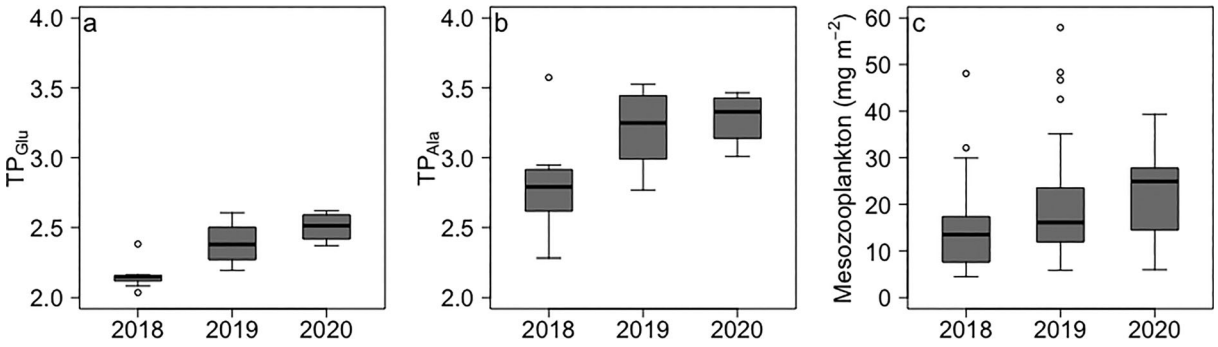

Fig. 8. Interannual comparisons of juvenile krill TP and mesozooplankton biomass. TP was calculated using (**a**) glutamic acid and (**b**) alanine as the trophic amino acid. (**c**) Mesozooplankton dry weight density was integrated from 0 to 50 m at Stas. B and E. Black line indicates the median, gray box indicates the interquartile range, and whiskers indicate the range excluding outlier values indicated as points. For (**a**) and (**b**), $n = 4$–10 samples per year. For (**c**), $n = 16$–61 samples per year.

in that study may have been higher due to the inclusion of larger juvenile animals (age-class 2) and were particularly elevated south of Palmer Station (Bernard et al. 2012). In contrast, our mean of 0.7 μg ind^{-1} d^{-1} was similar to measurements for juvenile krill in the eastern Atlantic sector at 56–60°S during December and January (range: 0.5–0.6 μg ind^{-1} d^{-1}) (Pakhomov and Froneman 2004). No significant change in grazing rate (and the order-of-magnitude decline in mass-specific grazing) over the size range considered in our study supported the use of a single functional response for krill from age-class 1. The positive relationship between grazing rate and Chl *a* concentration using gut fluorescence supported the use of a functional feeding response that we investigated more thoroughly in independent experiments.

Unlike in some prior studies, we found a functional response in our krill feeding experiments that indicates grazing saturates as Chl *a* concentration increases. This finding likely reflects the use of natural plankton communities at natural densities to mimic in situ prey conditions. Prior studies show grazing continues to increase at Chl *a* concentrations as high as ~ 20 μg L^{-1}, which may be due to artificial concentration of large prey (Price et al. 1988; Atkinson and Snÿder 1997; Meyer et al. 2010). At least one previous study also reported a type III functional response for *E. superba* (Boyd et al. 1984), and type III responses are expected for active feeders such as krill (Agersted and Nielsen 2016; Kiørboe et al. 2018), which seek out prey and reduce feeding effort in the absence of prey (Hamner et al. 1983). While clearance rates may be depressed within experimental containers (Price et al. 1988; and see Supplementary Discussion), our experimental volume (18 liters) was relatively high for a feeding study, and the small size of the animals in our study likely reduced container effects compared to prior work with adult krill.

Phytoplankton grazing (< 1–9% krill body carbon d^{-1}) was insufficient to meet juvenile krill carbon demand. Two previous studies measuring gut fluorescence found similar results. During January in the eastern Atlantic sector of the Southern Ocean, daily phytoplankton grazing was < 2% of krill body carbon except at a single ice-edge station where a bloom was underway (Perissinotto et al. 1997). In addition, mean daily

Table 1. Summary of juvenile krill trophic role and prey availability during three consecutive field seasons. Annual mean, standard deviation, and sample size (n) are reported for TP calculated using glutamic acid (TP_{Glu}) and alanine (TP_{Ala}). The annual mean and range of estimates are reported for dietary fractions, which should be considered exploratory due to substantial uncertainty. The carbon budget-based phytoplankton dietary fraction is derived from Fig. 5. Annual mean, standard deviation, and sample size are reported for Chl *a* and mesozooplankton dry weight measurements (integrated from 0 to 50 m) at Stas. B and E.

	2017–2018	2018–2019	2019–2020	Mean ($n = 3$ yr)
TP_{Glu}	2.2 ± 0.1 ($n = 9$)	2.4 ± 0.1 ($n = 10$)	2.5 ± 0.1 ($n = 4$)	2.3
TP_{Ala}	2.8 ± 0.4 ($n = 9$)	3.2 ± 0.3 ($n = 10$)	3.3 ± 0.2 ($n = 4$)	3.1
% Metazoans (stable isotopes)	14 (13–15)	35 (32–38)	46 (42–50)	32
% Heterotrophic protists (stable isotopes)	36 (25–55)	38 (21–56)	31 (14–44)	35
% Phytoplankton (stable isotopes)	50 (29–62)	27 (6–47)	22 (5–44)	33
% Phytoplankton (carbon budget)	23 (14–31)	26 (17–35)	22 (14–30)	24
Chl *a* (mg m^{-2})	67 ± 38 ($n = 76$)	96 ± 77 ($n = 84$)	69 ± 54 ($n = 58$)	77
Mesozooplankton dry weight (mg m^{-2})	14 ± 9 ($n = 40$)	19 ± 11 ($n = 61$)	23 ± 10 ($n = 16$)	19

phytoplankton grazing was 0.5% of body carbon for juvenile krill during January along the WAP (Bernard et al. 2012). At the high end, experimental incubations using sea-ice derived algae found that daily phytoplankton grazing was 10% of body carbon when C_{phyto} concentration was 600 $\mu g\ L^{-1}$ but dropped below 4% of body carbon at a C_{phyto} level of ~ 300 $\mu g\ L^{-1}$ (Meyer et al. 2010). Thus, our finding of inadequate phytoplankton consumption to support krill carbon demand is supported by previous studies and a range of methodologies.

There is a clear mismatch between the size-selectivity of krill and the natural size distribution of available autotrophic prey near Palmer Station. Imaging flow cytometry showed that > 60% of natural biovolume was concentrated in nano-sized particles that krill fed upon 50–75% less efficiently compared to larger particles. Small-celled phytoplankton persistently dominated across two field seasons at Palmer Station, and mean cell size decreased from late spring to early autumn (Nardelli et al. 2023). Our size-specific clearance rates (1–4.5 L $ind^{-1}\ d^{-1}$) also agree well with a previous experimental study of similarly sized krill (18–23 mm) and natural plankton prey that reports mean clearance rates of 1 L $ind^{-1}\ d^{-1}$ on prey < 20 μm and 2–3 L $ind^{-1}\ d^{-1}$ on prey > 20 μm (Meyer and El-Sayed 1983).

Trophic position and dietary composition

The seasonal carbon budget of krill growth, respiration, and grazing allowed calculation of a minimum feasible TP independent of stable isotope data. This carbon budget suggested phytoplankton comprised up to 35% seasonal carbon ingestion (Table 1). We then assumed the 65% of unaccounted prey occupy the minimum heterotrophic TP of 2 and calculated krill TP according to Pauly and Palomares (2005). The seasonal carbon budget thus suggests a minimum krill TP of 2.65.

The mean TP_{Ala} of juvenile krill was 3.1 ± 0.4 and reveals the importance of heterotrophic protists in the coastal Antarctic food web. TP_{Ala} exceeded 2.65 for 87% of samples while TP_{Glu} (mean = 2.3 ± 0.2) was always less than 2.65. Only alanine isotopically detects trophic steps through heterotrophic protists (Gutiérrez-Rodríguez et al. 2014; Décima et al. 2017), which are the dominant grazers in the WAP ecosystem (Garzio et al. 2013; Sailley et al. 2013). TP_{Ala} thus accounted for important trophic links and revealed that juvenile krill were secondary consumers during summer near Palmer Station. Substantial uncertainty remains when estimating TP from $\delta^{15}N$ of amino acids. For example, isotopic composition varies within individuals, and our use of muscle tissue likely elevated TP estimates compared to the entire krill body (Schmidt et al. 2004).

Two prior studies report amino acid $\delta^{15}N$ values for krill abdominal muscle, revealing regional and ontogenetic variability in food web structure. Krill in the Scotia Sea and near South Georgia during January–February had the highest ^{15}N enrichment in glutamic acid and alanine relative to phenylalanine (Schmidt et al. 2006) (Supplementary Fig. S11), possibly attributable to increased regional abundance of mesozooplankton prey (Yang et al. 2022) and the inclusion of larger krill, which occupy higher trophic levels (Polito et al. 2013). Female krill collected near the South Shetland Islands in late summer (March) exhibited higher relative ^{15}N enrichment in glutamic acid compared to alanine when both were normalized to $\delta^{15}N_{Phe}$ (Schmidt et al. 2004) (Supplementary Fig. S11), suggesting increased importance of metazoans relative to heterotrophic protists. This finding for adult krill is again consistent with an ontogenetic shift in TP relative to juvenile krill in our study.

Our carbon budget and stable isotope approaches both suggest heterotrophic prey were major dietary components in all years, particularly when mesozooplankton biomass was elevated. Heterotrophic material constituted on average 79% (standard deviation = 21%) of stomach content mass for krill collected in the Lazarev Sea (January) and near South Georgia (February–March) (Perissinotto et al. 2000). Much of the stomach contents of krill is visually unidentifiable, but heterotrophic protists can dominate the identified portion (Schmidt et al. 2006). Copepods are often relatively rare in identified

stomach contents (Schmidt et al. 2014) despite high experimental clearance rates when they are provided as prey for krill (Price et al. 1988; Atkinson and Snÿder 1997). Genetic diet analysis in the northern Antarctic Peninsula from March to May indicated that copepods (mainly *Oithona*, *Metridia*, and *Calanus* spp.) were the most common prey class in krill stomachs (27% of sequence reads), and that krill positively selected for copepods and assimilated them more efficiently than other prey (Pauli et al. 2021). Fatty acid trophic markers confirm that copepods are consistent prey for krill across regions and seasons (Schmidt et al. 2014); however, dietary fractions remain uncertain, and there is continued need to reconcile dietary information across various methods (Schmidt and Atkinson 2016).

Population-level implications

Current hypotheses underlying krill population dynamics should be re-evaluated within a framework that emphasizes omnivory. A simulation model including only autotrophic prey suggests that competition-driven starvation of larval and juvenile krill during autumn is the key driver of regional population cycles along the WAP (Ryabov et al. 2017). Our results also demonstrate that phytoplankton is insufficient to support juvenile krill from summer into autumn, but autumn starvation may be reduced when juvenile krill feed substantially on heterotrophic prey. Thus, future models should include heterotrophic prey. Empirical relationships show that larval abundance and subsequent recruitment are positively related to phytoplankton biomass (Loeb et al. 2009; Saba et al. 2014). One interpretation is that higher reproductive output and overwinter survival are due to increased phytoplankton (particularly diatom) consumption. We do not rule this out but note that elevated phytoplankton biomass also coincides with elevated abundance of heterotrophic prey, including copepods and microzooplankton (Loeb et al. 2009; Garzio and Steinberg 2013; Gleiber 2014). Unraveling the drivers of highly variable krill recruitment should inform regional krill fishery management (Meyer et al. 2020), which currently is insufficient to permit expansion or to protect dependent predators (Brooks et al. 2022; Watters and Hinke 2022).

Over multi-decadal scales, climate-driven changes in phytoplankton may be important direct and indirect drivers of shifting krill biogeography. As southern shelf waters of the WAP shifted from perennial to seasonal sea ice coverage from the 1990s to 2010s, phytoplankton biomass and cell size increased (Montes-Hugo et al. 2009; Rogers et al. 2020). Over the same period, an important krill spawning area developed in southern WAP waters (Atkinson et al. 2022). Years of extended sea-ice coverage and high, diatom-dominated productivity likely result in greater phytoplankton consumption by krill, because krill can most efficiently graze large diatoms that are specifically associated with ice-edge phytoplankton blooms (Lin et al. 2021). As sea ice continues to decline, phytoplankton biomass and cell size are expected to decrease in this region (Montes-Hugo et al. 2009; Brown et al. 2019; Rogers et al. 2020), likely increasing the number of trophic steps between phytoplankton and krill. The physiological impacts of changing krill diet composition require further study. For example, increased diatom consumption promotes immediate growth and reproduction while a copepod-rich diet favors longer-term storage for overwintering (Hagen et al. 2007; Bernard et al. 2022). Clarifying the connections from diet to physiology to population dynamics will inform krill fishery management amidst unprecedented environmental change.

Generality of findings

It is worth considering whether krill feasibly can be secondary consumers given their immense biomass in the high nutrient, low Chl *a* Southern Ocean. To do this, we compiled circumpolar productivity estimates of krill and their major prey (Supplementary Table S2; Supplementary Discussion). Annual krill productivity is 6–11% of combined microzooplankton plus calanoid copepod production (Supplementary Table S2). Given transfer efficiency between consumers is estimated at 3.5–25.5% (mean = 12%) in polar oceans (Eddy et al. 2021), krill could occupy a full trophic level above microzooplankton and copepods. Indeed, balanced food web models for South Georgia (Hill et al. 2012) and the northern WAP coast (Sailley et al. 2013) demonstrate krill could realistically feed on < 50% phytoplankton in both regions. But importantly, mean annual primary productivity along the coastal WAP (180 g C m^{-2} yr^{-1}) (Ducklow et al. 2013) is triple the Southern Ocean mean (57 g C m^{-2} yr^{-1}) (Arrigo et al. 2008), and thus our findings are specific to a region where increased phytoplankton production may allow krill to occupy a higher TP. In addition, krill can readily feed near the seafloor in shallow coastal regions where vertical migration is a less-effective escape mechanism for copepods (Atkinson et al. 1999; Schmidt et al. 2011). Therefore, krill could be secondary consumers throughout the Southern Ocean, but local conditions may make it more likely at our study site.

Conclusions

Heterotrophic prey surpassed phytoplankton contributions to juvenile krill diet across three summer field seasons near Palmer Station. Coastal waters are the most productive along the WAP (Vernet et al. 2008; Brown et al. 2019), phytoplankton productivity is highest during summer (Clarke et al. 2008), and juvenile krill are expected to rely less on omnivory compared to larger individuals (Polito et al. 2013; Schmidt et al. 2014). This local result was therefore surprising, and we posit that krill are secondary consumers more broadly. We thus encourage investigation into krill-centric food web structure at a circumpolar scale and across life stages. Controlled experimentation to define TEF values for the pelagic Antarctic food web would be valuable for re-analysis of our data and CSIA-AA data yet to be collected. A comparative, multi-taxa CSIA-AA approach could prove valuable, and data

may be harvested from frozen or preserved sample collections (Hetherington et al. 2019; Swalethorp et al. 2020). Time series would be particularly useful when paired with krill population demographics, physiological measurements, and prey data (Walsh et al. 2020; Steinke et al. 2021). Future studies should look beyond the phytoplankton–krill–predator food chain to interrogate complexity in the changing Southern Ocean food web.

Data availability statement

The data that support the findings of this study are available in the supplementary material of this article or will be made available in the Environmental Data Initiative Data Portal or at reasonable request of the corresponding author.

References

Agersted, M. D., and T. G. Nielsen. 2016. Functional biology of sympatric krill species. J. Plankton Res. **38**: 575–588. doi:10.1093/plankt/fbw017

Arrigo, K. R., G. L. van Dijken, and S. Bushinsky. 2008. Primary production in the Southern Ocean, 1997-2006. J. Geophys. Res. **113**: C08004. doi:10.1029/2007JC004551

Atkinson, A., and others. 2006. Natural growth rates in Antarctic krill (*Euphausia superba*): II. Predictive models based on food, temperature, body length, sex, and maturity stage. Limnol. Oceanogr. **51**: 973–987. doi:10.4319/lo.2006.51.2.0973

Atkinson, A., and others. 2022. Stepping stones towards Antarctica: Switch to southern spawning grounds explains an abrupt range shift in krill. Glob. Change Biol. **28**: 1359–1375. doi:10.1111/gcb.16009

Atkinson, A., and R. Snÿder. 1997. Krill-copepod interactions at South Georgia, Antarctica, I. Omnivory by *Euphausia superba*. Mar. Ecol. Prog. Ser. **160**: 63–76. doi:10.3354/meps160063

Atkinson, A., P. Ward, A. Hill, A. S. Brierley, and G. C. Cripps. 1999. Krill-copepod interactions at South Georgia, Antarctica, II. *Euphausia superba* as a major control on copepod abundance. Mar. Ecol. Prog. Ser. **176**: 63–79. doi:10.3354/meps176063

Båmstedt, U., D. J. Gifford, X. Irigoien, A. Atkinson, and M. Roman. 2000. Feeding, p. 297–399. *In* R. Harris, P. Wiebe, J. Lenz, H. R. Skjoldal, and M. Huntley [eds.], ICES zooplankton methodology manual. Academic. doi:10.1016/B978-012327645-2/50009-8

Belcher, A., and others. 2019. Krill faecal pellets drive hidden pulses of particulate organic carbon in the marginal ice zone. Nat. Commun. **10**: 889. doi:10.1038/s41467-019-08847-1

Bernard, K. S., D. K. Steinberg, and O. M. E. Schofield. 2012. Summertime grazing impact of the dominant macrozooplankton off the Western Antarctic peninsula. Deep-Sea Res. I Oceanogr. Res. Pap. **62**: 111–122. doi:10.1016/j.dsr.2011.12.015

Bernard, K. S., K. B. Steinke, and J. M. Fontana. 2022. Winter condition, physiology, and growth potential of juvenile Antarctic krill. Front. Mar. Sci. **9**: 990853. doi:10.3389/fmars.2022.990853

Boyd, C. M., M. Heyraud, and C. N. Boyd. 1984. Feeding of the Antarctic krill *Euphausia superba*. J. Crustacean Biol. **4**: 123–141. doi:10.1163/1937240X84X00543

Brooks, C. M., and others. 2022. Protect global values of the Southern Ocean ecosystem. Science **378**: 477–479. doi:10.1126/science.add9480

Brown, M. S., D. R. Munro, C. J. Feehan, C. Sweeney, H. W. Ducklow, and O. M. Schofield. 2019. Enhanced oceanic CO_2 uptake along the rapidly changing West Antarctic Peninsula. Nat. Clim. Change **9**: 678–683. doi:10.1038/s41558-019-0552-3

Chikaraishi, Y., and others. 2009. Determination of aquatic food-web structure based on compound-specific nitrogen isotopic composition of amino acids. Limnol. Oceanogr. Methods **7**: 740–750. doi:10.4319/lom.2009.7.740

Clarke, A., M. P. Meredith, M. I. Wallace, M. A. Brandon, and D. N. Thomas. 2008. Seasonal and interannual variability in temperature, chlorophyll and macronutrients in northern Marguerite Bay, Antarctica. Deep-Sea Res. II Top. Stud. Oceanogr. **55**: 1988–2006. doi:10.1016/j.dsr2.2008.04.035

Clarke, A., L. B. Quetin, and R. M. Ross. 1988. Laboratory and field estimates of the rate of faecal pellet production by Antarctic krill, *Euphausia superba*. Mar. Biol. **98**: 557–563. doi:10.1007/BF00391547

Conroy, J. A., D. K. Steinberg, M. I. Thomas, and L. T. West. 2023. Seasonal and interannual changes in a coastal Antarctic zooplankton community. Mar. Ecol. Prog. Ser. **706**: 17–32. doi:10.3354/meps14256

Décima, M., and M. R. Landry. 2020. Resilience of plankton trophic structure to an eddy-stimulated diatom bloom in the North Pacific Subtropical Gyre. Mar. Ecol. Prog. Ser. **643**: 33–48. doi:10.3354/meps13333

Décima, M., M. R. Landry, C. J. Bradley, and M. L. Fogel. 2017. Alanine $\delta^{15}N$ trophic fractionation in heterotrophic protists. Limnol. Oceanogr. **62**: 2308–2322. doi:10.1002/lno.10567

Ducklow, H. W., and others. 2013. West Antarctic Peninsula: An ice-dependent coastal marine ecosystem in transition. Oceanography **26**: 190–203. doi:10.5670/oceanog.2013.62

Eddy, T. D., and others. 2021. Energy flow through marine ecosystems: Confronting transfer efficiency. Trends Ecol. Evol. **36**: 76–86. doi:10.1016/j.tree.2020.09.006

Färber-Lorda, J., R. Gaudy, and P. Mayzaud. 2009. Elemental composition, biochemical composition and caloric value of Antarctic krill. Implications in energetics and carbon balances. J. Mar. Syst. **78**: 518–524. doi:10.1016/j.jmarsys.2008.12.021

Frost, B. W. 1972. Effects of size and concentration of food particles on the feeding behavior of the marine planktonic copepod *Calanus pacificus*. Limnol. Oceanogr. **17**: 805–815. doi:10.4319/lo.1972.17.6.0805

Fuentes, V., and others. 2016. Glacial melting: An overlooked threat to Antarctic krill. Sci. Rep. **6**: 27234. doi:10.1038/srep27234

Garzio, L. M., and D. K. Steinberg. 2013. Microzooplankton community composition along the Western Antarctic Peninsula. Deep-Sea Res. I Oceanogr. Res. Pap. **77**: 36–49. doi:10.1016/j.dsr.2013.03.001

Garzio, L. M., D. K. Steinberg, M. Erickson, and H. W. Ducklow. 2013. Microzooplankton grazing along the Western Antarctic Peninsula. Aquat. Microb. Ecol. **70**: 215–232. doi:10.3354/ame01655

Gleiber, M. R. 2014. Long-term change in copepod community structure in the Western Antarctic Peninsula: Linkage to climate and implications for carbon cycling. M.S. thesis. College of William & Mary.

Gleiber, M. R., D. K. Steinberg, and H. W. Ducklow. 2012. Time series of vertical flux of zooplankton fecal pellets on the continental shelf of the western Antarctic Peninsula. Mar. Ecol. Prog. Ser. **471**: 23–36. doi:10.3354/meps10021

Gutiérrez-Rodríguez, A., M. Décima, B. N. Popp, and M. R. Landry. 2014. Isotopic invisibility of protozoan trophic steps in marine food webs. Limnol. Oceanogr. **59**: 1590–1598. doi:10.4319/lo.2014.59.5.1590

Hagen, W., T. Yoshida, P. Virtue, S. Kawaguchi, K. M. Swadling, S. Nicol, and P. D. Nichols. 2007. Effect of a carnivorous diet on the lipids, fatty acids and condition of Antarctic krill, *Euphausia superba*. Antarct. Sci. **19**: 183–188. doi:10.1017/S0954102007000259

Hamner, W. M., P. P. Hamner, S. W. Strand, and R. W. Gilmer. 1983. Behavior of Antarctic krill, *Euphausia superba*: Chemoreception, feeding, schooling, and molting. Science **220**: 433–435. doi:10.1126/science.220.4595.433

Hetherington, E. D., C. M. Kurle, M. D. Ohman, and B. N. Popp. 2019. Effects of chemical preservation on bulk and amino acid isotope ratios of zooplankton, fish, and squid tissues. Rap. Commun. Mass Spectrom. **33**: 935–945. doi:10.1002/rcm.8408

Hewes, C. D., O. Holm-Hansen, and E. Sakshaug. 1985. Alternate carbon pathways at lower trophic levels in the Antarctic food web, p. 277–283. *In* W. R. Siegfried, P. R. Condy, and R. M. Laws [eds.]. Antarctic nutrient cycles and food webs. doi:10.1007/978-3-642-82275-9_40

Hill, S. L., K. Keeble, A. Atkinson, and E. J. Murphy. 2012. A foodweb model to explore uncertainties in the South Georgia shelf pelagic ecosystem. Deep Sea Res. II Topic. Stud. Oceanogr. **59–60**: 237–252. doi:10.1016/j.dsr2.2011.09.001

Hoen, D. K., S. L. Kim, N. E. Hussey, N. J. Wallsgrove, J. C. Drazen, and B. N. Popp. 2014. Amino acid ^{15}N trophic enrichment factors of four large carnivorous fishes. J. Exp. Mar. Biol. Ecol. **453**: 76–83. doi:10.1016/j.jembe.2014.01.006

Holling, C. S. 1965. The functional response of predators to prey density and its role in mimicry and population regulation. Mem. Entomol. Soc. Can. **97**: 5–60. doi:10.4039/entm9745fv

Holm-Hansen, O., and M. Huntley. 1984. Feeding requirements of krill in relation to food sources. J. Crustacean Biol. **4**: 156–173. doi:10.1163/1937240X84X00561

Ikeda, T., and B. Bruce. 1986. Metabolic activity and elemental composition of krill and other zooplankton from Prydz Bay, Antarctica, during early summer (November–December). Mar. Biol. **92**: 545–555. doi:10.1007/BF00392514

Kawaguchi, S., S. G. Candy, R. King, M. Naganobu, and S. Nicol. 2006. Modelling growth of Antarctic krill. I. Growth trends with sex, length, season, and region. Mar. Ecol. Prog. Ser. **306**: 1–15. doi:10.3354/meps306001

Kiørboe, T., F. Møhlenberg, and H. Nicolajsen. 1982. Ingestion rate and gut clearance in the planktonic copepod *Centropages hamatus* (Lilljeborg) in relation to food concentration and temperature. Ophelia **21**: 181–194. doi:10.1080/00785326.1982.10426586

Kiørboe, T., E. Saiz, P. Tiselius, and K. H. Andersen. 2018. Adaptive feeding behavior and functional responses in zooplankton. Limnol. Oceanogr. **63**: 308–321. doi:10.1002/lno.10632

Lin, Y., and others. 2021. Decline in plankton diversity and carbon flux with reduced sea ice extent along the Western Antarctic Peninsula. Nat. Commun. **12**: 4948. doi:10.1038/s41467-021-25235-w

Loeb, V. J., E. E. Hofmann, J. M. Klinck, O. Holm-Hansen, and W. B. White. 2009. ENSO and variability of the Antarctic Peninsula pelagic marine ecosystem. Antarct. Sci. **21**: 135–148. doi:10.1017/S0954102008001636

Marin, V., M. E. Huntley, and B. Frost. 1986. Measuring feeding rates of pelagic herbivores: Analysis of experimental design and methods. Mar. Biol. **93**: 49–58. doi:10.1007/BF00428654

Mauchline, J. 1980. Measurement of body length of *Euphausia superba* Dana. BIOMASS handbook, v. **4**. Cambridge: Scientific Committee on Antarctic Research; p. 1–9.

McMahon, K. W., and M. D. McCarthy. 2016. Embracing variability in amino acid δ^{15}N fractionation: Mechanisms, implications, and applications for trophic ecology. Ecosphere **7**: e01511. doi:10.1002/ecs2.1511

Meyer, B., A. Atkinson, B. Blume, and U. V. Bathmann. 2003. Feeding and energy budgets of larval Antarctic krill *Euphausia superba* in summer. Mar. Ecol. Prog. Ser. **257**: 167–178. doi:10.3354/meps257167

Meyer, B., and others. 2010. Seasonal variation in body composition, metabolic activity, feeding, and growth of adult krill *Euphausia superba* in the Lazarev Sea. Mar. Ecol. Prog. Ser. **398**: 1–18. doi:10.3354/meps08371

Meyer, B., and others. 2020. Successful ecosystem-based management of Antarctic krill should address uncertainties in krill recruitment, behaviour and ecological adaptation. Commun. Earth Environ. **1**: 28. doi:10.1038/s43247-020-00026-1

Meyer, M. A., and S. Z. El-Sayed. 1983. Grazing of *Euphausia superba* Dana on natural phytoplankton populations. Polar Biol. **1**: 193–197. doi:10.1007/BF00443187

Montes-Hugo, M., S. C. Doney, H. W. Ducklow, W. Fraser, D. Martinson, S. E. Stammerjohn, and O. Schofield. 2009. Recent changes in phytoplankton communities associated with rapid regional climate change along the Western Antarctic Peninsula. Science **323**: 1470–1473. doi:10.1126/science.1164533

Nardelli, S. C., P. C. Gray, S. E. Stammerjohn, and O. Schofield. 2023. Characterizing coastal phytoplankton seasonal succession patterns on the West Antarctic Peninsula. Limnol. Oceanogr. **68**: 845–861. doi:10.1002/lno.12314

Nicol, S., and J. Foster. 2016. The fishery for Antarctic krill: Its current status and management regime, p. 387–421. *In* V. Siegel [ed.], Biology and ecology of Antarctic krill. Springer.

Olson, R. J., and H. M. Sosik. 2007. A submersible imaging-in-flow instrument to analyze nano- and microplankton: Imaging FlowCytobot. Limnol. Oceanogr. Methods **5**: 195–203. doi:10.4319/lom.2007.5.195

Pakhomov, E. A., and P. W. Froneman. 2004. Zooplankton dynamics in the eastern Atlantic sector of the Southern Ocean during the austral summer 1997/1998—Part 2: Grazing impact. Deep-Sea Res. II Top. Stud. Oceanogr. **51**: 2617–2631. doi:10.1016/j.dsr2.2000.11.002

Pauli, N.-C., and others. 2021. Selective feeding in Southern Ocean key grazers—Diet composition of krill and salps. Commun. Biol. **4**: 1061. doi:10.1038/s42003-021-02581-5

Pauly, D., and M.-L. Palomares. 2005. Fishing down marine food web: It is far more pervasive than we thought. Bull. Mar. Sci. **76**: 197–211.

Perissinotto, R., L. Gurney, and E. A. Pakhomov. 2000. Contribution of heterotrophic material to diet and energy budget of Antarctic krill, *Euphausia superba*. Mar. Biol. **136**: 129–135. doi:10.1007/s002270050015

Perissinotto, R., E. A. Pakhomov, C. D. McQuaid, and P. W. Froneman. 1997. *In situ* grazing rates and daily ration of Antarctic krill *Euphausia superba* feeding on phytoplankton at the Antarctic Polar Front and the Marginal Ice Zone. Mar. Ecol. Prog. Ser. **160**: 77–91. doi:10.3354/meps160077

Polito, M. J., C. S. Reiss, W. Z. Trivelpiece, W. P. Patterson, and S. D. Emslie. 2013. Stable isotopes identify an ontogenetic niche expansion in Antarctic krill (*Euphausia superba*) from the South Shetland Islands, Antarctica. Mar. Biol. **160**: 1311–1323. doi:10.1007/s00227-013-2182-z

Price, H. J., K. R. Boyd, and C. M. Boyd. 1988. Omnivorous feeding behavior of the Antarctic krill *Euphausia superba*. Mar. Biol. **97**: 67–77. doi:10.1007/BF00391246

R Core Team. 2021. R: A language and environment for statistical computing. R Foundation for Statistical Computing. Available from: https://www.R-project.org/

Reiss, C. S. 2016. Age, growth, mortality, and recruitment of Antarctic krill, *Euphausia superba*, p. 101–144. *In* V. Siegel [ed.], Biology and ecology of Antarctic krill. Springer. doi:10.1007/978-3-319-29279-3_3

Rogers, A. D., and others. 2020. Antarctic futures: An assessment of climate-driven changes in ecosystem structure, function, and service provisioning in the Southern Ocean. Ann. Rev. Mar. Sci. **12**: 87–120. doi:10.1146/annurev-marine-010419-011028

Ruiz-Halpern, S., C. M. Duarte, A. Tovar-Sanchez, M. Pastor, B. Horstkotte, S. Lasternas, and S. Agustí. 2011. Antarctic krill as a source of dissolved organic carbon to the Antarctic ecosystem. Limnol. Oceanogr. **56**: 521–528. doi:10.4319/lo.2011.56.2.0521

Ryabov, A. B., A. M. de Roos, B. Meyer, S. Kawaguchi, and B. Blasius. 2017. Competition- induced starvation drives large-scale population cycles in Antarctic krill. Nat. Ecol. Evol. **1**: 0177. doi:10.1038/s41559-017-0177

Saba, G. K., and others. 2014. Winter and spring controls on the summer food web of the coastal West Antarctic Peninsula. Nat. Commun. **5**: 4318. doi:10.1038/ncomms5318

Sailley, S. F., H. W. Ducklow, H. V. Moeller, W. R. Fraser, O. M. Schofield, D. K. Steinberg, L. M. Garzio, and S. C. Doney. 2013. Carbon fluxes and pelagic ecosystem dynamics near two western Antarctic peninsula Adélie penguin colonies: An inverse model approach. Mar. Ecol. Prog. Ser. **492**: 253–272. doi:10.3354/meps10534

Schmidt, K., and A. Atkinson. 2016. Feeding and food processing in Antarctic krill (*Euphausia superba* Dana), p. 175–224. *In* V. Siegel [ed.], Biology and ecology of Antarctic krill. Springer. doi:10.1007/978-3-319-29279-3_5

Schmidt, K., A. Atkinson, K.-J. Petzke, M. Voss, and D. W. Pond. 2006. Protozoans as a food source for Antarctic krill, *Euphausia superba*: Complementary insights from stomach content, fatty acids, and stable isotopes. Limnol. Oceanogr. **51**: 2409–2427. doi:10.4319/lo.2006.51.5.2409

Schmidt, K., A. Atkinson, D. W. Pond, and L. C. Ireland. 2014. Feeding and overwintering of Antarctic krill across its major habitats: The role of sea ice cover, water depth, and phytoplankton abundance. Limnol. Oceanogr. **59**: 17–36. doi:10.4319/lo.2014.59.1.0017

Schmidt, K., J. W. McClelland, E. Mente, J. P. Montoya, A. Atkinson, and M. Voss. 2004. Trophic-level interpretation based on $\delta^{15}N$ values: Implications of tissue-specific fractionation and amino acid composition. Mar. Ecol. Prog. Ser. **266**: 43–58. doi:10.3354/meps266043

Schmidt, K., and others. 2011. Seabed foraging by Antarctic krill: Implications for stock assessment, bentho-pelagic coupling, and the vertical transfer of iron. Limnol. Oceanogr. **56**: 1411–1428. doi:10.4319/lo.2011.56.4.1411

Schofield, O., and others. 2017. Decadal variability in coastal phytoplankton community composition in a changing West Antarctic Peninsula. Deep-Sea Res. I Oceanogr. Res. Pap. **124**: 42–54. doi:10.1016/j.dsr.2017.04.014

Shelton, A. O., D. Kinzey, C. Reiss, S. Munch, G. Watters, and M. Mangel. 2013. Among-year variation in growth of Antarctic krill *Euphausia superba* based on length-frequency data. Mar. Ecol. Prog. Ser. **481**: 53–67. doi:10.3354/meps10245

Siegel, V., and V. Loeb. 1994. Length and age at maturity of Antarctic krill. Antarct. Sci. **6**: 479–482. doi:10.1017/S0954102094000726

Sosik, H. M., and R. J. Olson. 2007. Automated taxonomic classification of phytoplankton sampled with imaging-in-flow cytometry. Limnol. Oceanogr. Methods **5**: 205–216. doi:10.4319/lom.2007.5.204

Steinke, K. B., K. S. Bernard, R. M. Ross, and L. B. Quetin. 2021. Environmental drivers of the physiological condition of mature female Antarctic krill during the spawning season: Implications for krill recruitment. Mar. Ecol. Prog. Ser. **669**: 65–82. doi:10.3354/meps13720

Swadling, K. M., D. A. Ritz, S. Nicol, J. E. Osborn, and L. J. Gurney. 2005. Respiration rate and cost of swimming for Antarctic krill, *Euphausia superba*, in large groups in the laboratory. Mar. Biol. **146**: 1169–1175. doi:10.1007/s00227-004-1519-z

Swalethorp, R., L. Aluwihare, A. R. Thompson, M. D. Ohman, and M. R. Landry. 2020. Errors associated with compound-specific δ^{15}N analysis of amino acids in preserved fish samples purified by high-pressure liquid chromatography. Limnol. Oceanogr. Methods **18**: 259–270. doi:10.1002/lom3.10359

Trathan, P. N., and S. L. Hill. 2016. The importance of krill predation in the Southern Ocean, p. 321–350. *In* V. Siegel [ed.], Biology and ecology of Antarctic krill. Springer. doi:10.1007/978-3-319-29279-3_9

Vernet, M., D. Martinson, R. Iannuzzi, S. Stammerjohn, W. Kozlowski, K. Sines, R. Smith, and I. Garibotti. 2008. Primary production within the sea-ice zone west of the Antarctic Peninsula: I—Sea ice, summer mixed layer, and irradiance. Deep-Sea Res. II Top. Stud. Oceanogr. **55**: 2068–2085. doi:10.1016/j.dsr2.2008.05.021

Walsh, J., C. S. Reiss, and G. M. Watters. 2020. Flexibility in Antarctic krill *Euphausia superba* decouples diet and recruitment from overwinter sea-ice conditions in the northern Antarctic Peninsula. Mar. Ecol. Prog. Ser. **642**: 1–19. doi:10.3354/meps13325

Walsh, R. G., S. He, and C. T. Yarnes. 2014. Compound-specific δ^{13}C and δ^{15}N analysis of amino acids: A rapid, chloroformate-based method for ecological studies. Rapid Commun. Mass Sptrom. **28**: 96–108. doi:10.1002/rcm.6761

Watters, G. M., and J. T. Hinke. 2022. Conservation in the Scotia Sea in light of expiring regulations and disrupted negotiations. Conserv. Biol. **36**: e13925. doi:10.1111/cobi.13925

Yang, G., A. Atkinson, E. A. Pakhomov, S. L. Hill, and M.-F. Racault. 2022. Massive circumpolar biomass of Southern Ocean zooplankton: Implications for food web structure, carbon export, and marine spatial planning. Limnol. Oceanogr. **67**: 2516–2530. doi:10.1002/lno.12219

Yarnes, C. T., and J. Herszage. 2017. The relative influence of derivatization and normalization procedures on the compound-specific stable isotope analysis of nitrogen in amino acids. Rapid Commun. Mass Spectrom. **31**: 693–704. doi:10.1002/rcm.7832

Acknowledgments

Thank you to the Antarctic Support Contract personnel at Palmer Station for their scientific and logistical support. We thank Andrew Corso, Ashley Hann, Kharis Schrage, Leigh West, Rachael Young, and PAL LTER colleagues for their contributions to this field project. Comments from Kim Bernard, David Johnson, Walker Smith, Mike Vecchione, and three anonymous reviewers improved this manuscript. This work was supported by the National Science Foundation Antarctic Organisms and Ecosystems Program (PLR-1440435 and OPP-2026045) and student research grants from the William & Mary. J.A.C. was supported in part under award 724071 (Virginia Sea Grant Project V724070) from the National Oceanic and Atmospheric Administration (NOAA). The statements, findings, conclusions, and recommendations are those of the authors and do not necessarily reflect the views of Virginia Sea Grant, NOAA, or the U.S. Department of Commerce.

Conflict of interest

The authors have no conflicts of interest to declare.

Submitted 07 April 2023
Revised 29 September 2023
Accepted 03 February 2024

Associate editor: Thomas Kiørboe